DOI: 10.7860/JCDR/2026/84092.22277

Original Article

Pharmacology Section

Exploring the Antifibrotic Potential of *Vitex negundo* Compounds via Molecular Docking, Molecular Dynamics and ADMET Profiling: An In-silico Analysis

K AKILANDEESHWARI[1], D ANUSHA[2], K PRIYA GAYATHRI[3], KAVITHA RAMASAMY[4]

ABSTRACT

Introduction: Fibrosis is the excessive accumulation of extracellular matrix in tissues due to abnormal wound healing, leading to organ dysfunction and high morbidity and mortality across multiple organs. *Vitex negundo* L. (Verbenaceae), commonly known as the Chinese chaste tree or "Huangjing," is an aromatic shrub native to South and Southeast Asia, China, Japan, and East Africa. It is widely recognised in traditional medicine systems for its diverse pharmacological actions. The plant exhibits anti-inflammatory, antioxidant, antifibrotic, hepatoprotective, and antimicrobial properties. These effects are primarily attributed to its rich phytochemical constituents, such as luteolin, casticin, and negundoside. Owing to its multifaceted bioactivity, *Vitex negundo* serves as a promising source for the development of novel therapeutic agents.

Aim: To evaluate the antifibrotic potential of *Vitex negundo* bioactive compounds through in-silico methods, including molecular docking, molecular dynamics, and ADMET (Absorption, Distribution, Metabolism, Excretion and Toxicity) profile analysis, focusing on their interaction with key fibrotic signaling pathways.

Materials and Methods: This in-silico analysis was conducted in the Department of Pharmacology, Sri Ramachandra Medical College, Chennai, Tamil Nadu, India, over a period of one month, from June 2025 to July 2025. The study focused on the molecular docking of casticin, luteolin, and negundoside with TGFβR1 and SMAD3. Optimised ligand and protein structures were sourced from public databases, and ADMET properties were predicted using SWISSADME and ProTox 3.0. Molecular docking (AutoDock Vina) and visualisation (PyMOL) were used to assess binding, while 100 ns molecular dynamics simulations (AMBER ff19SB) evaluated complex stability using Root Mean Square Deviation (RMSD), Principal Component Analysis (PCA), and Molecular Mechanics/Generalised Born Surface Area (MM/GBSA) binding energy calculations.

Results: Casticin, luteolin, and negundoside from *Vitex negundo* showed strong binding to TGFβR1 and moderate to strong binding to SMAD3, with casticin having the highest affinities. Molecular dynamics confirmed stable, rigid protein-ligand complexes for casticin and luteolin. ADMET analysis indicated high gastrointestinal absorption and low toxicity for all three compounds; however, casticin and luteolin may cause drug-drug interactions due to Cytochrome P450 (CYP) inhibition, while negundoside showed lower absorption but minimal metabolic risk.

Conclusion: *Vitex negundo* demonstrates significant anti-inflammatory, antioxidant, and antifibrotic activities. These findings support its potential as a safe and effective therapeutic agent with anti-inflammatory properties, justifying further investigation into its antifibrotic activity.

Keywords: Bioactive compounds, Fibrosis, Phytochemical

INTRODUCTION

Fibrosis is characterised by the excessive accumulation of fibrous connective tissue, resulting in the disruption of normal tissue architecture and impaired organ function. This pathological condition can affect various organs, including the lungs, liver, kidneys, and heart, and often progresses to life-threatening stages if left untreated. Fibrosis is a common feature of chronic inflammatory diseases and can arise from persistent tissue injury, oxidative stress, or autoimmune conditions [1].

The fibrotic process is primarily driven by the activation of fibroblasts and the excessive deposition of extracellular matrix (ECM) components, such as collagen and fibronectin. Among the key regulators of this process, the Transforming Growth Factor-beta (TGFβ) signaling pathway plays a pivotal role. TGFβ, through its receptors (TGFβR1 and TGFβR2), activates downstream effectors like SMAD2/3 proteins, leading to the transcription of profibrotic genes [1, 2]. Dysregulation of this pathway has been implicated in the initiation and progression of fibrosis across multiple organ systems. Targeting TGFβ signaling components, particularly TGFβR1 and SMAD3, has therefore emerged as a promising therapeutic strategy to mitigate fibrosis [3].

Current antifibrotic therapies, while representing significant progress, remain limited in their ability to fully address the burden of fibrotic diseases. Most approved treatments, such as pirfenidone and nintedanib, have been approved only for idiopathic pulmonary fibrosis and focus on slowing disease progression rather than reversing established fibrosis. These treatments are often specific to certain organs or underlying causes. Emerging strategies in antifibrotic therapy increasingly focus on both shared and organ-specific mechanisms [3].

Currently, there are no approved antifibrotic drugs that directly and specifically target the TGFβ-SMAD pathway, even though this pathway is a central driver of fibrosis in organs such as the liver, kidney, heart, and lungs. The complexity and redundancy of fibrotic signaling networks, along with individual variability in treatment response, highlight the urgent need for new therapies that are more precise, effective, and better tolerated [4].

Recent research is exploring a range of promising strategies to inhibit the TGFβ-SMAD pathway. Experimental compounds such as

imidazole-based ALK5 inhibitors, miglustat, and natural products like Bruceine A and parthenolide have shown the ability to block TGFβ-SMAD signaling and reduce fibrosis in preclinical models of liver, lung, heart, and kidney disease [5]. These agents work by interfering with key steps in the pathway, such as blocking receptor activation or preventing the phosphorylation and nuclear translocation of SMAD proteins. However, these therapies are still in the experimental or early clinical stages and are not yet available for routine clinical use [6].

The development of targeted TGFβ-SMAD inhibitors with broad organ applicability and improved safety profiles remains a top priority. As research advances, these new agents may offer more effective and personalised options for patients with fibrotic diseases, moving beyond the limitations of existing treatments that only slow disease progression and often cause significant side-effects.

Vitex negundo, commonly known as the Chinese chaste tree, is a medicinal plant widely used in traditional systems of medicine, including Ayurveda and Chinese medicine. This plant has been recognised for its diverse pharmacological properties, including anti-inflammatory and antioxidant activities [7]. Phytochemical analysis, including Gas Chromatography-Mass Spectrometry (GC-MS), has identified several bioactive compounds in *Vitex negundo*, such as casticin, luteolin, and negundoside. These compounds are known to exhibit significant biological activities, including interactions with molecular targets involved in inflammation and fibrosis [7,8].

Emerging evidence suggests that the antifibrotic potential of these bioactives may be attributed to their ability to modulate the TGFβ signaling pathway. By inhibiting key proteins such as TGFβR1 and SMAD3, these compounds could attenuate fibroblast activation and ECM accumulation [8]. However, the molecular mechanisms underlying these interactions remain to be fully elucidated.

This study aimed to investigate the antifibrotic potential of casticin, luteolin, and negundoside derived from *Vitex negundo*. Using an in-silico approach, molecular docking will be employed to predict the binding interactions of these compounds with TGFβ signaling proteins. Additionally, molecular dynamics simulations will be conducted to assess the stability of these interactions, and ADMET analyses will be performed to evaluate their drug-likeness and safety profiles. The findings of this study could provide valuable insights into the potential of these bioactives as therapeutic agents for managing fibrosis and offer a scientific basis for their further development in antifibrotic drug discovery [9].

MATERIALS AND METHODS

This in-silico analysis was conducted in the Department of Pharmacology at Sri Ramachandra Medical College, Chennai Tamil Nadu, India, over a period of one month, from June 2025 to July 2025. The study protocol was reviewed by the Institutional Ethics Committee (IEC), with approval number CSP-MED/25/MAY/115/90.

Methodology: The study focused on the molecular docking of casticin, luteolin, and negundoside with TGFβR1 and SMAD3. Optimised structures were retrieved from PubChem and the Protein Data Bank. Ligands and targets were refined, and ADMET properties such as absorption and toxicity were predicted using SWISSADME and ProTox 3.0. Molecular docking was performed using AutoDock Vina, and PyMOL was used to visualise key interactions. Molecular dynamics simulations were conducted over 100 ns using the AMBER ff19SB force field to assess complex stability through RMSD and PCA analyses, followed by MM/GBSA calculations to estimate binding affinities.

Protein preparation: The study investigated the antifibrotic potential of the bioactive compounds casticin, luteolin, and negundoside. Their 3D structures were obtained from PubChem and optimised for docking studies using Open Babel and AutoDockTools. TGFβ receptor type 1 (TGFβR1) and SMAD3, key proteins in the TGFβ signaling pathway, were retrieved from the Protein Data Bank (PDB IDs: 6B8Y and 1MK2) and prepared by removing water molecules, adding polar hydrogens, and refining the structures.

Protocol for docking studies: ADMET properties, such as solubility, lipophilicity, and gastrointestinal absorption, were analysed using SwissADME, while ProTox 3.0 predicted toxicity profiles, including hepatotoxicity and LD50 values. AutoDock Vina was employed for molecular docking to identify binding affinities and key interactions, which were visualised using PyMOL and Discovery Studio Visualiser. Molecular dynamics simulations were carried out for 100 nanoseconds using the OpenMM framework and AMBER ff19SB force field, evaluating the stability and flexibility of ligand-protein complexes through parameters such as Root Mean Square Deviation (RMSD), Root Mean Square Fluctuation (RMSF), and Principal Component Analysis (PCA).

RESULTS

Casticin and its interactions with SMAD3 and TGFβR1: Casticin displayed a binding energy of -5.5 kcal/mol with SMAD3, where interactions were predominantly stabilised by hydrogen bonds with ASN338 and ARG322, along with hydrophobic contacts involving PHE303 and ASN343. These interactions suggest that casticin binds effectively within the binding site of SMAD3, potentially disrupting its fibrotic signaling pathway. Additionally, casticin showed strong binding to TGFβR1, with a binding energy of -9.2 kcal/mol. The key residues involved in this interaction included hydrogen bonds with GLU341 and hydrophobic interactions with ASN259 and HIS283, indicating a high binding affinity that supports its potential as a TGFβR1 antagonist in the context of fibrosis [Table/Fig-1].

Casticin's ADMET profile: From a pharmacokinetic perspective, casticin exhibited high gastrointestinal absorption and moderate lipophilicity (Log P=2.5), which may contribute to its favourable bioavailability. The compound did not cross the Blood-Brain Barrier (BBB), suggesting limited central nervous system effects. Furthermore, casticin inhibited key CYP enzymes (CYP1A2, CYP2C9, CYP3A4), which may increase the likelihood of drug-drug interactions in clinical settings [Table/Fig-2,3]. Toxicity testing revealed an LD50 of >5000 mg/kg, categorising it as practically non toxic (Toxicity Class 5) [Table/Fig-4].

Luteolin and its interactions with SMAD3 and TGFβR1: Luteolin demonstrated a binding energy of -4.3 kcal/mol with SMAD3, forming hydrogen bonds with TYR223 and ILE278, accompanied by hydrophobic interactions with ILE308. This suggests a moderate binding affinity to SMAD3, which may allow luteolin to modulate SMAD3-mediated fibrotic signaling. Additionally, luteolin bound strongly to TGFβR1, showing a binding energy of -8.0 kcal/mol. The primary interactions involved hydrogen bonds with ARG371 and hydrophobic contacts with ILE211 and LEU278, suggesting that luteolin could act as a potent inhibitor of TGFβR1, which plays a pivotal role in fibrosis progression [Table/Fig-1].

Luteolin's ADMET profile: Luteolin exhibited high gastrointestinal absorption and moderate lipophilicity (Log P=1.73), supporting its potential bioavailability. It was not found to cross the blood-BBB, indicating that its effects are likely confined to peripheral tissues. Luteolin also inhibited CYP enzyme (CYP1A2) suggesting that it may interfere with the metabolism of other drugs, posing a potential risk for metabolic interactions [Table/Fig-2,3]. In toxicity testing, luteolin presented an LD50 of 3919 mg/kg, classifying it as practically non toxic (Toxicity Class 5) [Table/Fig-4].

Negundoside and its interactions with SMAD3 and TGFβR1: Negundoside demonstrated a lower binding affinity for SMAD3, with a binding energy of -3.9 kcal/mol. The interaction was primarily stabilised by weak hydrogen bonds with ASN338 and PHE303, indicating a relatively weaker interaction compared to casticin and luteolin. This suggests that further structural modifications could improve its efficacy against SMAD3. However, negundoside exhibited a stronger binding affinity for TGFβR1, with a binding

energy of -8.7 kcal/mol. Key residues involved in this interaction included hydrogen bonds with ASN259 and GLU341, highlighting negundoside's selective affinity for TGFβR1, a crucial receptor in the fibrotic cascade [Table/Fig-1].

Negundoside's ADMET profile: Negundoside exhibited low gastrointestinal absorption and negligible lipophilicity (Log P=-0.33), which may limit its systemic availability. It did not cross the BBB, reducing the likelihood of central nervous system side-effects (Table/Fig-2,3). Moreover, negundoside did not significantly inhibit CYP enzymes, suggesting a lower risk for metabolic interactions. Toxicity testing revealed an LD50 of 2000 mg/kg, classifying it as practically non-toxic (Toxicity Class 4) [Table/Fig-4].

Complex		Binding energy (kcal/mol)
Casticin	SMAD3	-5.5
	TFGβR1	-9.2
Luteolin	SMAD3	-4.3
	TFGβR1	-8.0
Negundoside	SMAD3	-3.9
	TFGβR1	-8.7

[Table/Fig-1]: Binding energy values of all the complexes during molecular docking analysis.

	Property	Casticin	Luteolin	Negundoside
Physicochemical properties	Formula	C19H18O8	C15H10O6	C23H28O12
	Molecular Weight	374.34 g/mol	286.24 g/mol	496.46 g/mol
	No. of heavy atoms	27	21	35
	No. of aromatic heavy atoms	16	16	6
	No. of rotatable bonds	5	1	7
	No. of H-Bond acceptors	8	6	12
	No. of H-Bond donors	2	4	6
Log P (Lipophilicity)	Log *Po*/w	2.5	1.73	-0.33
Water solubility (mg/ml)	Log S Solubility Class	-5.43 1.38e-03 Moderately soluble	-3.82 4.29e-02 soluble	0.07 5.87e+02 Highly soluble
Pharmacokinetics	GI Absorption	High	High	Low
	BBB Permeation	No	No	No
	P-gp Substrate	No	No	No
	CYP1A2 Inhibitor	Yes	Yes	No
	CYP2C19 Inhibitor	No	No	No
	CYP2C9 Inhibitor	Yes	No	No
	CYP2D6 Inhibitor	No	No	No
	CYP3A4 Inhibitor	Yes	No	No
	Log Kp (Skin Permeation)	-6.37 cm/s	-6.25 cm/s	-9.39 cm/s
Drug likeliness	Bioavailability score	0.55	0.55	0.11
	Lipinski's rule of five	Yes	Yes	No

[Table/Fig-2]: ADME properties of casticin, luteolin, and negundoside.

Molecular Dynamics Analysis of Casticin: Binding Energy, Stability, Flexibility, and Conformational Behaviour

1. The Binding Energy

The binding free energy of casticin, calculated via MM-PBSA, was -43.1 kcal/mol, indicating favourable and stable protein-ligand interactions. This stability was largely driven by Van der Waals interactions (-49.2 kcal/moL) and electrostatic contributions (-36.4 kcal/mol). Gas-phase energy (ΔGgas: -85.6 kcal/mol) further reinforced the interaction, while solvation energy (ΔGsolv: 42.5 kcal/mol) slightly offset the binding affinity [Table/Fig-5].

Complex		Hydrogen bonding interactions	Hydrophobic interactions
Casticin	SMAD3 Dock	Phe303 (2.9), Arg322 (2.8), Tyr323 (2.2), Asn338 (2.2), Leu339 (2.3), Lys340 (2.1), Asn343 (2.8)	Phe303 (5.3), Tyr323 (5.3), Lys340 (3.9)
	TFGβR1 Dock	Ile211 (2.4), Lys232 (1.8), Glu245 (1.8), Leu278 (2.6), Ser280 (2.7), His283 (1.6), Leu340 (2.6), Asp351 (2.3),	Ile211 (3.8), Val219 (5.0), Lys232 (4.6), Tyr249 (3.7), Leu260 (4.6), Leu278 (4.0), Leu340 (4.7), Ala350 (4.4)
	MD	Leu81 (2.1), Val219 (3.1), Ala230 (2.9), Glu245 (1.9), Tyr249 (1.9), Tyr282 (2.5), Tyr283 (2.0), Gly286 (3.6), Lys337 (2.2), Asp351 (2.1)	Ile211 (3.9), Val219 (4.5), Lys232 (4.3), Tyr249 (4.0), Leu260 (4.2), Ala350 (5.0)
Luteolin	SMAD3 Dock	Phe303 (3.1), Arg322 (1.8), Tyr323 (2.6), Asn338 (1.9), Leu339 (2.5), Lys340 (2.0), Asn343 (2.0)	Phe303 (5.7), Lys340 (3.7)
	TFGβR1 Dock	Ile211 (3.3), Val219 (3.1), Ala230 (3.3), Lys232 (2.0), Glu245 (2.2), Ser280 (2.1), Tyr282 (2.5), His283 (2.1), Leu340 (3.3), Asp351 (2.0)	Ile211 (4.7), Val219 (4.9), Ala230 (3.9), Lys232 (5.0), Leu260 (4.6), Leu340 (3.6), Ala350 (4.9)
	MD	His86 (2.7), Gly89 (2.5), Ser90 (3.5), Asp93 (3.5), Ile211 (3.0), Val219 (2.7), Lys232 (2.5), Glu245 (1.9), Leu260 (3.0), Leu278 (3.2), Asp281 (3.2), Tyr282 (3.2), Leu340 (2.9), Ala350 (2.4), Asp351 (1.5)	Val219 (2.8), Ala230 (4.5), Lys232 (4.1), Leu260 (4.9), Leu340 (4.4), Ala350 (5.2),
Negundoside	SMAD3 Dock	Phe303 (2.1), Arg322 (2.5), Tyr323 (2.1), Asn338 (2.1), Lys340 (2.6), Arg343 (2.4)	Leu339 (5.2)
	TFGβR1 Dock	Ile211 (3.1), Lys213 (2.9), Val219 (2.4), Lys232 (2.9), Ser280 (2.9), Asp281 (2.6), His283 (2.1), Gly286 (3.0), Ala350 (2.2), Asp351 (2.4),	Ile211 (5.0), Val219 (4.6), Ala230 (4.0), Leu340 (4.8)

[Table/Fig-3]: Intermolecular interactions (Å) of casticin, luteolin and negundoside compounds with SMAD3 and TGFβR1 proteins.

2. Stability: RMSD and Radius of Gyration (Rg)

The stability of the casticin-protein complex was evaluated using Root Mean Square Deviation (RMSD) and Radius of Gyration (Rg) analyses. The RMSD graph (a) displayed an initial equilibration phase during the first ~20 ns, after which the system stabilised with RMSD values consistently ranging between 1.0 and 2.0 Å. This indicates minimal deviations from the starting structure and reflects a strong, stable interaction between casticin and the protein binding site. The Rg graph (c) further confirmed this stability, showing values maintained within a narrow range of 19.3 to 19.6 Å throughout the 100 ns simulation. This steady range reflects a compact and well-organised structure, with no significant unfolding or major structural rearrangements. Together, these metrics highlight the stable dynamics of the protein-ligand complex under physiological conditions [Table/Fig-6].

3. Flexibility: RMSF and DCCM

The Root Mean Square Fluctuation (RMSF) graph (b) provided residue-specific insights into protein flexibility. Regions corresponding to loops and solvent-exposed segments displayed higher RMSF peaks, indicating localised flexibility, whereas core residues—particularly those in the binding pocket—exhibited consistently low RMSF values (~0.5–1.0 Å). This pattern underscores the rigidity of the binding pocket, which is essential for maintaining strong interactions with casticin while allowing slight flexibility in peripheral regions for functional adaptability.

CASTICIN

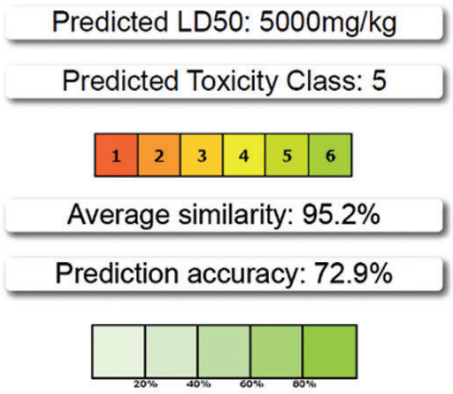

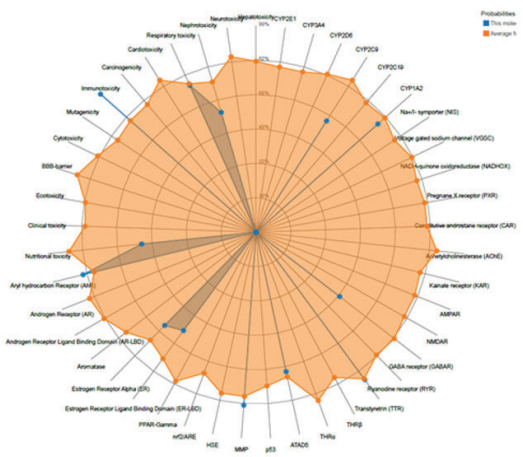

LUTEOLIN

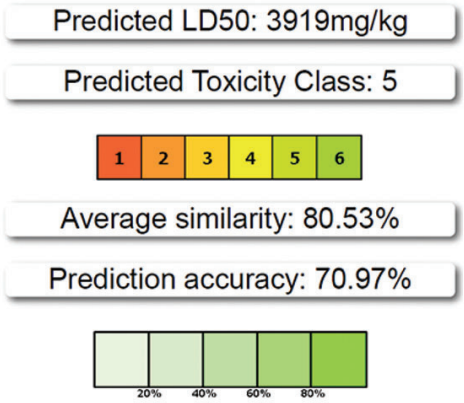

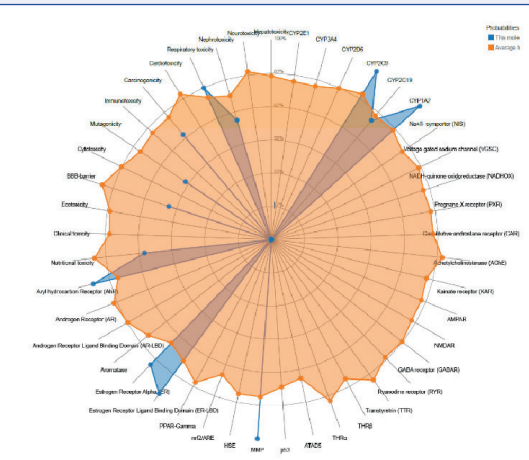

NEGUNDOSIDE

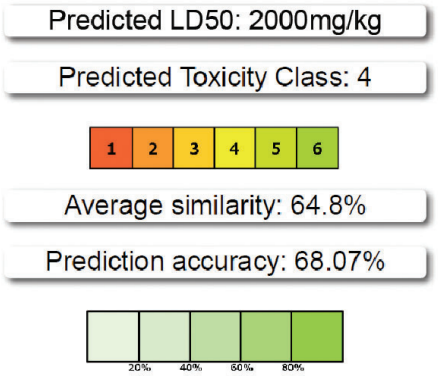

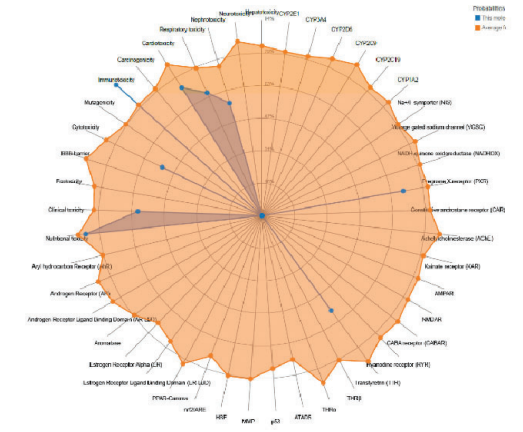

[Table/Fig-4]: Toxicity profile.

	VdW	EEL	EGB	ESURF	ΔΔGgas	ΔΔGsolv	ΔΔG Bind
Casticin	-49.2	-36.4	49.0	-6.6	-85.6	42.5	-43.1
Luteolin	-36.7	-34.8	44.3	-5.3	-71.4	38.9	-32.4

[Table/Fig-5]: MMGBSA binding free energy of casticin and luteolin-TGFβR1 enzyme complex
VdW – Van der Waals energy, EEL- Electrostatic energy, EGB- Electrostatic solvation energy(generalised born), ESURF- Nonpolar solvation energy (Surface Area), ΔGgas- Gas-phase free energy, ΔGsolv- Solvation free energy, ΔG Bind- Binding free energy

Dynamic Cross-Correlation Matrix (DCCM) analysis: The Dynamic Cross-Correlation Matrix (DCCM) plot (d) provided a comprehensive view of residue motion correlations. Positive correlations (green regions) were prominent in the binding pocket and nearby structural domains, indicating coordinated motions that stabilise the ligand interaction. In contrast, anti-correlated motions (pink regions) in distant areas reflect functional adaptability, which may assist in accommodating ligand-induced conformational changes without disrupting overall stability [Table/Fig-6].

Conformational sampling: Principal Component Analysis (PCA) and Distribution Plots: PCA offered critical insights into the conformational dynamics of the complex. The PCA scatter plot (e), mapping the first two principal components (PC1 and PC2), revealed a tightly clustered set of points, indicating limited conformational variability and restricted sampling of structural states during the 100 ns simulation. This finding demonstrates the dominance of stable conformations, with no significant transitions to alternate states. The PCA distribution plots (f) further validated these observations, displaying sharp and well-defined peaks for both PC1 and PC2. These peaks signify that the system predominantly occupies a few stable conformational states, reinforcing the structural rigidity and stability of the complex. This restricted sampling of conformational

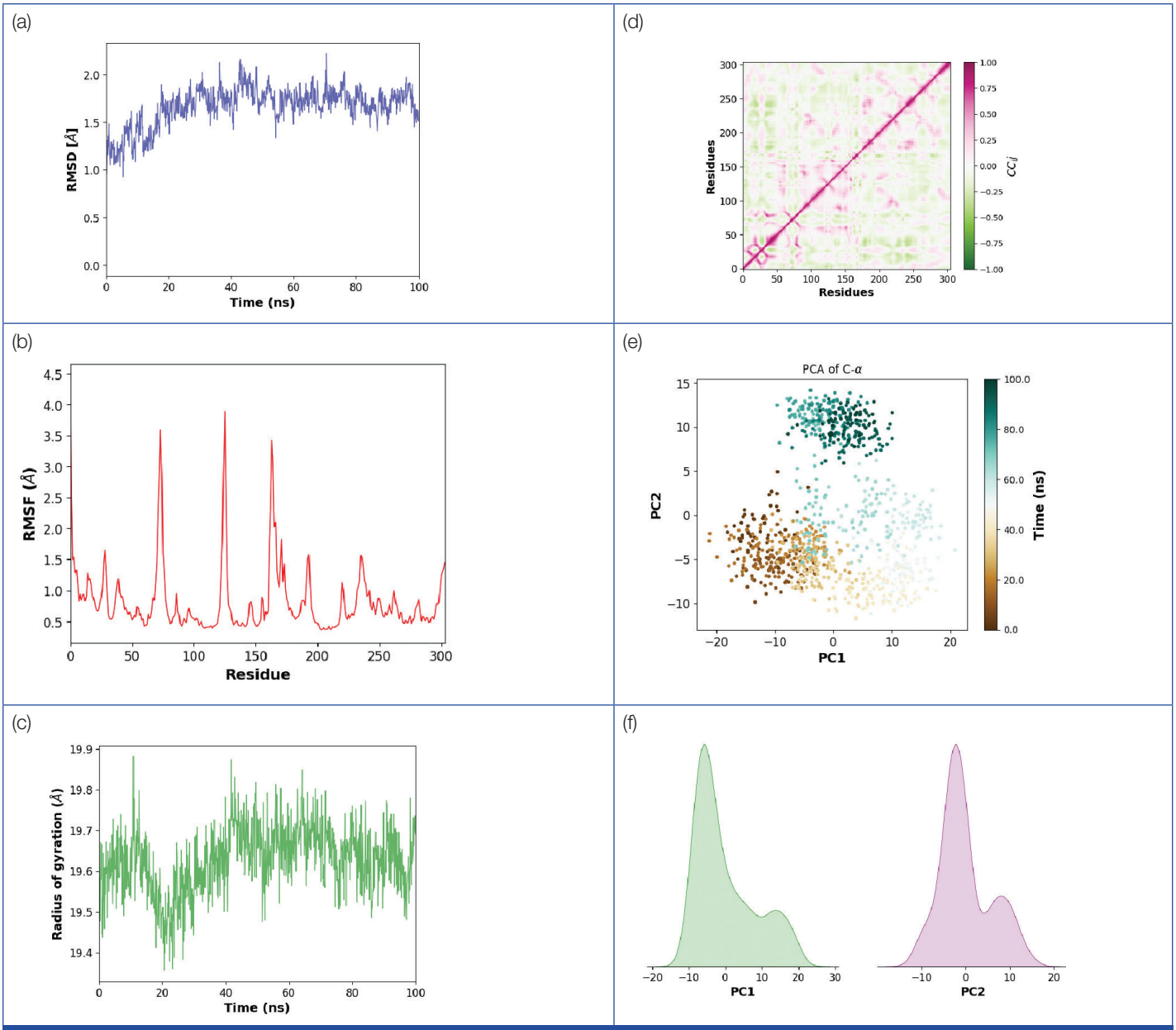

[Table/Fig-6]: Molecular dynamics of casticin
(A)RMSD, (B)RMSF, (C)Radius of Gyration, (D) DCCM, (E) PCA and (F) PCA distribution plots of Casticin TGFβR1 enzyme complexes.

space suggests a robust and energetically favourable protein-ligand interaction [Table/Fig-6].

Molecular Dynamics Analysis of Luteolin

1. Binding energy

The binding free energy of luteolin, calculated using MM-PBSA, was -32.4 kcal/mol, indicating favourable binding with the protein. This binding was primarily driven by Van der Waals interactions (-36.7 kcal/mol) and electrostatic energy contributions (-34.8 kcal/mol). The gas-phase energy (ΔGgas: -71.4 kcal/mol) reinforced the interaction, while solvation energy (ΔGsolv: 38.9 kcal/mol) slightly counteracted it [Table/Fig-5].

2. Stability: RMSD and Radius of Gyration (Rg)

The Root Mean Square Deviation (RMSD) graph (a) showed stabilisation after approximately 20 ns, with RMSD values remaining between 1.0 and 1.75 Å for the remainder of the 100 ns simulation. This consistency indicates minimal structural deviations and a robust protein-ligand interaction. The Radius of Gyration (Rg) graph (c) provided further confirmation of stability, showing values fluctuating between 19.3 and 19.6 Å. This narrow range indicates a compact protein structure, further validating the stable dynamics of the luteolin-protein complex [Table/Fig-7].

3. Flexibility: RMSF and DCCM

The Root Mean Square Fluctuation (RMSF) graph (b) revealed limited flexibility in key residues within the binding pocket, with RMSF values in these regions consistently low (approximately 0.5–1.0 Å). In contrast, higher RMSF peaks were observed in loop regions and solvent-exposed areas, reflecting localised flexibility that allows functional adaptability without compromising the stability of the binding site. The Dynamic Cross-Correlation Matrix (DCCM) plot (d) illustrated the inter-residue motion correlations. Positive correlations (green regions) were observed between residues in the binding site and adjacent domains, ensuring coordinated dynamics to maintain the ligand interaction. Anti-correlated motions (pink regions) in peripheral areas suggested dynamic adjustments to accommodate luteolin while preserving the structural integrity of the protein [Table/Fig-7].

4. Conformational Sampling: PCA and Distribution Plots

PCA provided insights into the conformational dynamics of the complex. The PCA scatter plot (e) revealed clustering along PC1 and PC2, indicating limited conformational variability and restricted sampling of conformational states over the 100 ns simulation. This suggests that the luteolin-protein complex maintains a consistent structural arrangement. The PCA distribution plots (f) for PC1 and PC2 demonstrated distinct peaks, reflecting dominant

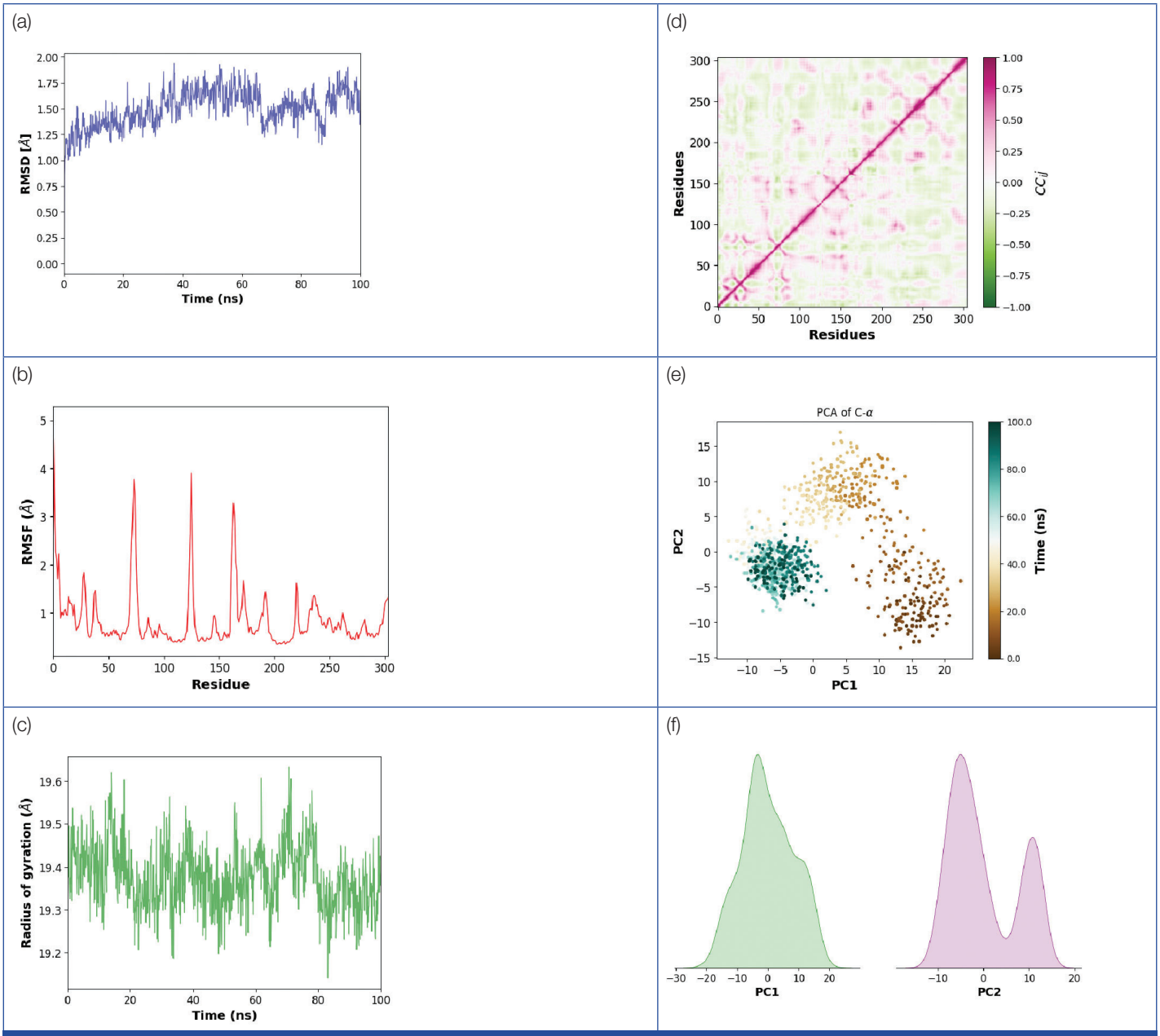

[Table/Fig-7]: Molecular dynamics of luteolin

conformational states that were repeatedly sampled during the simulation. These findings support the hypothesis that the luteolin-protein complex exhibits a stable dynamic profile, with limited transitions to alternative states [Table/Fig-7].

Consideration of negundoside: Negundoside was not subjected to molecular dynamics simulations in this study due to its low predicted oral bioavailability, as indicated by its high polarity, large molecular weight, and multiple sugar moieties. These factors suggest limited absorption and systemic exposure. In contrast, casticin and luteolin exhibit higher bioavailability scores and more favourable drug-like properties, making them more suitable candidates for detailed molecular dynamics analysis.

DISCUSSION

The present in-silico study explored the antifibrotic potential of *Vitex negundo*–derived bioactives, specifically casticin, luteolin, and negundoside, targeting the TGF-β/SMAD signaling pathway, which is recognised as a central driver of fibrogenesis across multiple organs. These results demonstrated strong and stable interactions of these ligands with TGFβR1 and SMAD3, as confirmed by molecular docking, 100-ns molecular dynamics simulations, and MM/GBSA free energy analyses. This suggests possible inhibitory effects on receptor activation and downstream Smad transduction.

These computational findings align with the experimental observations of Zhang Y et al., [10], who reported that luteolin markedly inhibited hepatic stellate cell proliferation and reduced Smad2/3 phosphorylation and collagen synthesis in rat models of CCl_4-induced hepatic fibrosis. This confirms its suppressive role on both Smad-dependent and Smad-independent profibrotic signaling. Similarly, Wu YT et al., [11] demonstrated that luteolin attenuated vascular smooth muscle cell proliferation and migration by directly inhibiting TGFβR1 phosphorylation and Smad2/3 activation, suggesting that luteolin may act as a receptor-level inhibitor. This strongly corroborates the docking data showing high binding affinity and hydrogen bond formation with catalytic residues within the ATP-binding domain of TGFβR1.

Comparable mechanistic evidence exists for casticin. Zhou L et al., [12] demonstrated that casticin attenuated liver fibrosis in both in vitro hepatic stellate cells (LX-2) and in-vivo CCl_4-induced models by blocking TGF-β1/Smad signaling and reducing the expression of α-SMA, collagen I, MMP-2, and TIMP-1. Lam HYP et al., [13] further reported that casticin exhibited antifibrotic and antiparasitic effects in *Schistosoma mansoni*–infected mice, decreasing hepatic TGF-β, α-SMA, and collagen type I expression. This computational analysis revealed that casticin demonstrated stable binding conformations to both TGFβR1 and SMAD3, low RMSD fluctuations during the MD

simulation, and favourable MM/GBSA binding energies, indicating thermodynamically stable complexes that could underpin the inhibitory activity observed experimentally.

The current literature on negundoside is largely limited to phytochemical characterisation, as reported by Dhanapal SS et al., [14], who confirmed its isolation and structural identity from ethanol leaf extracts of *V. negundo* using HPTLC and FTIR. However, its biological effects remain underexplored. In this study, negundoside exhibited stable binding to SMAD3 and favourable predicted ADMET parameters, including good intestinal absorption, non hepatotoxicity, and low predicted toxicity (ProTox-II class IV), suggesting potential as a safe antifibrotic candidate. This provides the first computational insight into its plausible molecular mechanism against fibrosis, meriting further in-vitro validation.

The antioxidant and anti-inflammatory profile of *V. negundo* supports this mechanistic plausibility. Kadir FA et al., [15] demonstrated that the ethanolic leaf extract of *V. negundo* protected against thioacetamide-induced liver fibrosis by normalising ALT, AST, and histological parameters. Tirpude NV et al., [16] found that *V. negundo* attenuated lung fibrosis and inflammation in a murine asthma model by modulating the AMPK/PI3K/Akt/p38-NF-κB and TGF-β/Smad pathways. Together, these studies indicate that the phytochemicals of *V. negundo* act through both redox and cytokine modulation, reducing oxidative stress, suppressing proinflammatory cytokines, and preventing myofibroblast activation—all of which are crucial early events in fibrogenesis.

Compared to these experimental reports, the in-silico findings add molecular precision by identifying specific amino acid residues involved in ligand–receptor binding and quantifying dynamic stability through RMSD and PCA analyses. The combined ADMET prediction further strengthens translational potential, showing that all three ligands possess high gastrointestinal absorption, non carcinogenic and non mutagenic properties, and acceptable drug-likeness scores according to SWISSADME. The dual mechanism—direct interference with the TGF-β/Smad axis and indirect mitigation of oxidative and inflammatory stress—offers a comprehensive explanation for the antifibrotic potential of *V. negundo* phytoconstituents [17].

Collectively, this computational study supports the growing body of evidence from Zhang Y et al., Wu YT et al., Zhou L et al., Lam HYP et al., Kadir FA et al., Tirpude NV et al., and Sivapalan S et al., [10-13,15-17]. It extends this understanding by introducing negundoside as a novel lead compound for future in-vitro and in-vivo antifibrotic investigations. These findings provide significant insights into the interaction of these compounds with key proteins of the TGF-β signaling pathway, which plays a central role in fibrosis progression (Hu HH, et al., [18] Wang W, et al., [19]). Previous in-vitro studies demonstrated the antioxidant and anti-inflammatory activities of *Vitex negundo* methanolic leaf extract, further supporting its therapeutic potential in managing inflammation and oxidative stress (Anusha S et al., 2019) [20].

Casticin demonstrated the strongest antifibrotic potential among the tested compounds. Docking results revealed high binding affinities for SMAD3 and TGFβR1, the primary proteins involved in the TGFβ signaling cascade. Its interactions were stabilised by critical hydrogen bonds and hydrophobic contacts, suggesting that casticin effectively binds within the active sites of these proteins, potentially disrupting their roles in fibroblast activation and ECM accumulation. The molecular dynamics simulations reinforced these findings by showing that casticin maintained stable protein-ligand complexes with minimal structural deviations over the simulation period. Furthermore, the calculated binding free energies confirmed strong and favourable interactions, which are essential for developing potent inhibitors of fibrosis-related pathways.

Luteolin exhibited moderate antifibrotic activity, with notable binding affinities to SMAD3 and TGFβR1. While its interaction energies were slightly weaker than those of casticin, luteolin demonstrated stability during MD simulations, indicating its potential to interfere with key signaling mechanisms in fibrosis. The ADMET analysis supported luteolin's therapeutic promise, revealing high gastrointestinal absorption and minimal toxicity risks. This makes luteolin a suitable candidate for further investigation, particularly for its potential role in combination therapies targeting multiple fibrotic mechanisms.

Negundoside, although less effective in binding to SMAD3, displayed strong interactions with TGFβR1, highlighting its selective antifibrotic action. While its docking and binding energy values were relatively lower compared to casticin and luteolin, negundoside's stability with TGFβR1 suggests that it could serve as a promising lead compound, particularly if optimised for better pharmacokinetic properties. However, negundoside's ADMET profile revealed lower gastrointestinal absorption and poor lipophilicity, which may limit its systemic bioavailability. Nonetheless, its low toxicity and minimal risk of metabolic interactions present opportunities for further chemical modification to improve its efficacy.

The ADMET analysis for all three compounds emphasised their suitability for therapeutic development. Casticin and luteolin exhibited high bioavailability and favourable drug-like properties, such as high gastrointestinal absorption and low toxicity. None of the compounds were predicted to cross BBB, which aligns with their intended peripheral action and minimises the risk of neurological side-effects. Notably, the low toxicity profiles, as indicated by LD50 values, further support the safety of these bioactive compounds for therapeutic applications.

Overall, this study underscores the potential of *Vitex negundo* bioactive compounds, particularly casticin, as effective antifibrotic agents targeting the TGFβ pathway. These findings are consistent with prior research highlighting the antifibrotic and anti-inflammatory properties of plant-derived compounds in modulating pathological signaling pathways. The robust molecular interactions, combined with favorable ADMET properties, provide a strong foundation for further preclinical evaluation.

Future directions for research: Future research should focus on validating these findings through in-vitro and in-vitro studies to assess the biological efficacy of these compounds in fibrotic disease models. Additionally, structural optimisation of negundoside and further exploration of combination therapies could enhance the therapeutic potential of these compounds.

Limitation(s)

While this study highlights the promising antifibrotic potential of *Vitex negundo* bioactive compounds—casticin, luteolin, and negundoside—through in-silico analysis, it is important to recognise a few limitations. The results are based purely on computational models, such as molecular docking, molecular dynamics simulations, and ADMET predictions. Although these tools are powerful for understanding molecular interactions, they cannot completely mimic the complexity of biological systems. The protein structures used were derived from crystallographic databases, which represent static snapshots and may not fully reflect the flexible, dynamic nature of proteins inside living cells.

The simulation period, though adequate for preliminary molecular insights, might not capture long-term conformational or stability changes that could influence actual biological activity. Moreover, the ADMET and toxicity profiles predicted through online platforms are theoretical and should be validated experimentally to confirm pharmacokinetic behaviour and safety. Another limitation was that the study does not include in-vitro or in-vitro experiments to confirm the computational predictions, such as whether these compounds truly inhibit TGF-β/Smad signaling, reduce collagen deposition, or suppress fibroblast activation.

Environmental factors like pH, ionic strength, and protein–protein interactions—which play significant roles in biological activity—were

also not simulated. Additionally, while compounds like casticin and luteolin have some experimental evidence supporting their antioxidant and anti-inflammatory actions, data on negundoside's specific antifibrotic potential remain scarce, limiting a complete comparative understanding.

In short, while the findings provide a strong theoretical foundation, experimental validation through in-vitro assays and in vivo fibrosis models is essential to translate these computational predictions into meaningful therapeutic evidence.

CONCLUSION(S)

This study demonstrated the antifibrotic potential of *Vitex negundo* bioactives, particularly casticin, luteolin, and negundoside, through their ability to interact with key proteins in the TGFβ signaling pathway, such as TGF-β1, TGF-β receptor I (TGFBR1), SMAD2, and SMAD3. Molecular docking and dynamics analyses revealed strong and stable interactions, especially for casticin, with promising ADMET profiles supporting their potential as drug candidates. These findings provide a foundation for further research into the development of safe and effective antifibrotic therapies.

Acknowledgement

The authors extend their sincere gratitude to the Department of Pharmacology, Sri Ramachandra Medical College and Research Institute, for their unwavering support, guidance, and encouragement throughout this study.

REFERENCES

[1] Ramadoss R, Sathish S, Sohn H, Madhavan T. Potency of anti-fibrotic herbs on fibrogenesis: A theoretical evaluation. Phytomed Plus. 2023;3(4):100496. Available from: https://doi.org/10.1016/j.phyplu.2023.100496.
[2] Xu H, Qu J, Wang J, Han K, Li Q, Bi W, et al. Discovery of pulmonary fibrosis inhibitor targeting TGF-β RI in Polygonum cuspidatum by high resolution mass spectrometry with in silico strategy. J Pharm Anal. 2022;12(6):860– 68. Available from: https://doi.org/10.1016/j.jpha.2020.05.006.
[3] Chen F, Lyu L, Xing C, Chen Y, Hu S, Wang M, et al. The pivotal role of TGF-β/Smad pathway in fibrosis pathogenesis and treatment. Front Oncol. 2025;15:1649179.
[4] Rockey DC, Weymouth N, Fabris L. Targeting TGF-β in fibrotic disease. Cell Mol Gastroenterol Hepatol. 2021;11(5):1471–85.
[5] Wang SQ, Meng YQ, Wu YL, Liu JJ, Zhao XY, Chen Y, et al. Imidazole-based ALK5 inhibitor attenuates TGF-β/Smad-mediated hepatic stellate cell activation and hepatic fibrogenesis. Chem Res Toxicol. 2025;38(5):930–41. doi:10.1021/acs.chemrestox.5c00036. Available from: https://pubmed.ncbi.nlm.nih.gov/40211771/.
[6] Iwanaga T, Chiba T, Nakamura M, Kaneko T, Ao J, Qiang N, Iwanaga J, et al. Miglustat, a glucosylceramide synthase inhibitor, mitigates liver fibrosis through TGF-β/Smad pathway suppression in hepatic stellate cells. Biochem Biophys Res Commun. 2023;642:192-200.
[7] Vishwanathan AS, Basavaraju R. A review on *Vitex negundo* L. – A medicinally important plant. East J Basic Sci. 2010;3(1):30–42.
[8] Zheng CJ, Li HQ, Ren SC, Xu CL, Rahman K, Qin LP, et al. Phytochemical and pharmacological profile of Vitex negundo. Phytother Res. 2015;29(5):633–47. doi:10.1002/ptr.5303.
[9] Nyamweya B, Omwaka P, Wanyama F. Cardioprotective effects of *Vitex negundo*: A review of mechanisms and clinical perspectives. J Complement Integr Med. 2023;20(1):1–12. Available from: https://doi.org/10.1177/2515690X23117662.
[10] Zhang Y, Li C, Li H, Song Y, Zhao L, Wang H, et al. Flavones hydroxylated at 5, 7, 3′ and 4′ ameliorate skin fibrosis by inhibiting Smad2/3 phosphorylation. Cell Death Dis. 2019;10(10):745.
[11] Wu YT, Chen L, Tan ZB, Fan HJ, Xie LP, Zhang WT, et al. Luteolin inhibits vascular smooth muscle cell proliferation and migration by suppressing TGF-βR1 signaling. Front Pharmacol. 2018;9:1059. Doi: 10.3389/fphar.2018.01059. PMID: 30298006; PMCID: PMC6160560.
[12] Zhou L, Dong X, Wang L, Shan L, Li T, Xu W, et al. Casticin attenuates liver fibrosis and hepatic stellate cell activation by blocking TGF-β/Smad signaling pathway. Oncotarget. 2017;8(34):56267–80. doi:10.18632/oncotarget.17453. PubMed PMID: 28915589.
[13] Lam HYP, Liang TR, Lan YC, Chang KC, Cheng PC, Peng SY. Antifibrotic and anthelminthic effect of casticin on Schistosoma mansoni-infected BALB/c mice. J Microbiol Immunol Infect. 2022 ;55(2):314-22. Doi: 10.1016/j.jmii.2021.03.017. Epub 2021 Jun 12. PMID: 34167886.
[14] Dhanapal SS, Balachandran P, Ranganathan S. HPTLC and FTIR studies on iridoid glycoside (Negundoside) isolated from ethanol leaf extracts of *Vitex negundo* Linn. Afr J Biomed Res. 2024;27(3):432–43.
[15] Kadir FA, Kassim NM, Abdulla MA, Yehye WA. Hepatoprotective role of ethanolic extract of *Vitex negundo* in thioacetamide-induced liver fibrosis in male rats. Evid Based Complement Alternat Med. 2013;2013:739850. Doi:10.1155/2013/739850. PubMed PMID: 23762157.
[16] Tirpude NV, Sharma A, Joshi R, Kumari M, Acharya V. *Vitex negundo* Linn. extract alleviates inflammatory aggravation and lung injury by modulating AMPK/PI3K/Akt/p38-NF-κB and TGF-β/Smad/Bcl-2/caspase/LC3 cascades. J Ethnopharmacol. 2021;268:113555. Doi:10.1016/j.jep.2020.113555. PubMed PMID: 33516930.
[17] Sivapalan S, Dharmalingam S, Ashokkumar V, Venkatesan V, Angappan M. Evaluation of the anti-inflammatory and antioxidant properties of Vitex negundo aqueous leaf extract. J Ethnopharmacol. 2024;319(Pt 3):117314. Ddoi: 10.1016/j.jep.2023.117314. Epub 2023 Oct 11. PMID: 37832812.
[18] Hu HH, Chen DQ, Wang YN, Feng YL, Cao G, Vaziri ND, et al. New insights into TGF-β/Smad signaling in tissue fibrosis. Chem Biol Interact. 2018;292:76-83.
[19] Wang W, Gao Y, Chen Y, Cheng M. TGF-β inhibitors: The future for prevention and treatment of liver fibrosis? Front Immunol. 2025;16:1583616.
[20] Anusha S, Rajesh SS, Priya AJ. In-vitro antioxidant and anti-inflammatory activities of methanolic leaf extract of Vitex negundo Linn. J Pharm Phytochem. 2019;8(4):1143–48.

PARTICULARS OF CONTRIBUTORS:
1. Postgraduate Student, Department of Pharmacology, Sri Ramachandra Medical College and Research Institute, Chennai, Tamil Nadu, India.
2. Professor, Department of Pharmacology, Sri Ramachandra Medical College and Research Institute, Chennai, Tamil Nadu, India.
3. Senior Resident, Department of Pharmacology, Sri Ramachandra Medical College and Research Institute, Chennai, Tamil Nadu, India.
4. Professor and Head, Department of Pharmacology, Sri Ramachandra Medical College and Research Institute, Chennai, Tamil Nadu, India.

NAME, ADDRESS, E-MAIL ID OF THE CORRESPONDING AUTHOR:
Dr. D Anusha,
No. 1, Mount Poonamallee Road, Ramachandra Nagar, Chennai-600116,
Tamil Nadu, India.
E-mail: anusha.d@sriramachandra.edu.in

PLAGIARISM CHECKING METHODS: [Jain H et al.]
- Plagiarism X-checker: Sep 22, 2025
- Manual Googling: Oct 23, 2025
- iThenticate Software: Oct 25, 2025 (9%)

ETYMOLOGY: Author Origin

EMENDATIONS: 7

AUTHOR DECLARATION:
- Financial or Other Competing Interests: None
- Was Ethics Committee Approval obtained for this study? Yes
- Was informed consent obtained from the subjects involved in the study? No
- For any images presented appropriate consent has been obtained from the subjects. No

Date of Submission: **Sep 03, 2025**
Date of Peer Review: **Oct 10, 2025**
Date of Acceptance: **Oct 27, 2025**
Date of Publishing: **Jan 01, 2026**